INTERNATIONAL JOURNAL OF AUTOMOTIVE AND MECHANICAL ENGINEERING
ISSN: 2229-8649 e-ISSN: 2180-1606
VOL. 21, ISSUE 3, 2024, 11695 – 11711
DOI: https://doi.org/10.15282/ijame.21.3.2024.19.0902

RESEARCH ARTICLE

# Fatigue Life and Stress Analysis of a Single Cylinder Four Stroke Crankshaft

**G. Jayanthan*, S.A. Abu Bakar and I.I. Mazali**

Faculty of Mechanical Engineering, Universiti Teknologi Malaysia, Johor Bahru, 81310 Skudai, Johor, Malaysia

**ABSTRACT –** This paper focuses on the optimization of a crankshaft using ANSYS software in terms of weight and strength. The initial designs of the crankshaft, piston, and connecting rod were created using SolidWorks. The force generated by the gas during the combustion process was calculated to be 12017 N. Next, the SolidWorks assembled system was imported into ADAMS View software for simulation, which revealed a time-variant force of the crankpin of 14049 N. The calculated value was verified with results obtained from analytical calculations, showing a deviation of 0.23%. Finite element analysis was done for the crankshaft using ANSYS transient structural after applying loadings and boundary conditions. The optimization process aimed to minimize the crankshaft's weight while maintaining its strength and durability. The results of the ANSYS simulations showed a weight reduction of 2.5% from the original 2.983 kg to 2.907 kg, while maintaining the required strength and durability. The optimized crankshaft was compared to its original design in terms of fatigue life, weights, and stresses. The maximum von Mises stress was reduced by 16%, shear stress by 3.5%, and deformation by 3.5%, which were validated through analytical calculations. The crankshaft analysis resulted in a significant increase in fatigue life, calculated to be infinite under the given conditions. To conclude, the objective to optimize the crankshaft for performance and efficiency was achieved, demonstrating a 2.5% weight reduction and substantial improvements in fatigue life and stress distribution, proving the effectiveness of ANSYS software for the design optimization process.

**ARTICLE HISTORY**
Received : 26th Sept. 2023
Revised : 22nd June 2024
Accepted : 13th Aug. 2024
Published : 24th Sept. 2024

**KEYWORDS**
*Crankshaft*
*Fatigue life*
*Finite element*
*ADAMS view*
*Weight optimization*

## 1. INTRODUCTION

The cranktrain is an important part of an engine with complex geometry, consisting of connecting rods, a crankshaft, pistons, and a flywheel. The main function of the crankshaft is to convert the reciprocating motion of the piston into the rotary motion of the crankshaft, which plays a major role in the automotive engine. Therefore, when designing a crankshaft, its fatigue performance and durability should be taken into account due to the large amount of load cycles it experiences during its service life [1,2,3]. The proper functioning of automotive engines often hinges on the performance and durability of the crankshaft. While prior research has provided valuable insights into crankshaft design and performance, it's crucial to recognize the limitations of existing optimization methods. Numerous studies have been done to explore the causes of crankshaft fatigue failure. For instance, M. Fonte et al. [4] analyzed two damaged crankshafts and identified fatigue fracture as the primary reason for failure due to bending. Similarly, K. Aliakbari et al. [5] investigated crankshaft failures in a six-cylinder diesel engine and identified the oil impurities and inappropriate machining as primary causes of fatigue cracks.

Mallikarjuna et al. [6] examined fatigue behavior, stress variations, and magnitudes at critical locations of crankshafts made of forged steel materials. They noted that the maximum deformation occurred at the center of the crankpin neck surface, the highest stress appeared at the fillets, and the high-stress area was at the edge of the main journal. Subsequently, Manpreet et al. [7] conducted a comparative study on the effects of deformations and stresses in four different materials, concluding that alloy steel induced the least stress and structural steel experienced the least deformation. One of the main challenges in ensuring optimal crankshaft performance is dealing with dynamic forces. The gas force generated during the combustion process within the engine cylinders not only propels the piston but is also influenced by factors like inertia and gravity [8]. The connecting rod transfers this force to the crankpin, initiating the crankshaft's rotation. Therefore, the crankpin must possess sufficient strength and durability to handle these dynamic forces effectively.

Three-dimensional modeling of crankshafts has been undertaken by various researchers employing different software, including SolidWorks, CATIA, AUTOCAD, and PRO-E [9–12]. Since experimental testing is not available, this section primarily focuses on computer modeling and reasonable stress analysis. Additionally, finite analysis has been conducted using software such as ANSYS and HYPERMESH [13–15]. Gopal et al. [16] investigated the efficiency of pistons, crankshafts, and connecting rods, revealing that stresses increase while displacements decrease when high alloy steel is used for the crankshaft. Maximum deformation is observed at the center of the crankpin surface [17,18]. Nandkumar et al. [19] discussed the use of von Mises stress, shear stress, fatigue life, safety factors, and sensitivity analysis in evaluating crankshaft performance. Von Mises stress and shear stress are used to identify areas of high stress concentration, while fatigue life determines the expected lifespan of the crankshaft. Safety factors ensure that the component design meets the required safety standards. Sensitivity analysis determines the crankshaft's lifecycle by analyzing how variations in

***CORRESPONDING AUTHOR | G. Jayanthan** | ✉ jayanthan@graduate.utm.my

crankpin diameters affect its performance. Based on these finite element analysis (FEA) results, it can be determined whether the design meets the required strength and stiffness criteria.

Optimization involves refining the design, conducting computer simulations, and reducing weight to achieve specific objectives, such as enhancing fatigue life, lowering material costs, or improving efficiency. Crankshaft design modifications can involve material removal to enhance performance characteristics. For instance, Thejasree et al. [20] focused on modeling and analyzing a crankshaft for a passenger car, achieving a 12.8% reduction in the crankshaft's weight compared to the original design. Reducing the crankshaft's weight can enhance engine performance, often achieved by using lightweight materials. Ramnath, B.V. et al. [21] conducted a comparative analysis of three different crankshaft materials, namely forged steel, ductile cast iron, and aluminum alloy. Based on the FEA results, forged steel is the most suitable material, with optimization resulting in an 18% reduction in its weight. Overall, optimization is a multifaceted process necessitating careful consideration of various factors, including material selection, design modifications, and operating conditions.

Pradhan et al. [22] conducted a finite element analysis and an analytical study of a four-stroke gasoline engine piston assembly. They validated the FEA results by performing analytical stress calculations, including computations related to connecting rod masses, crank angular velocity, and piston forces. Analytical stress calculations were conducted to verify the FEA results, and the outcomes were subsequently compared. Nevertheless, the methodologies used by previous researchers require further refinement to effectively address the intricacies of crankshaft optimization. Hence, this research aims to bridge this gap by employing a holistic approach. This approach begins by creating a detailed three-dimensional (3D) model of a four-stroke single-cylinder crankshaft using SolidWorks. Subsequently, ADAMS View is utilized to calculate the crankpin force and conduct an extensive finite element analysis (FEA) through ANSYS software. The ADAMS View simulation encompasses details of the kinematics of the components, the types of joints, the forces acting on the system, the inertia of the components, and the dynamic response of the system.

The primary objectives of this paper are to develop a 3D model of a crankshaft for a single-cylinder engine, investigate the original and modified crankshaft models using the same boundary conditions to optimize their fatigue life and explore design parameters that affect crankshaft performance. This analysis specifically involves a 3D model of a single-cylinder, four-stroke crankshaft. Both the original and modified crankshaft models are assessed using identical boundary conditions. Design parameters that influence crankshaft performance are also investigated and subsequently optimized in this paper.

## 2. COMPREHENSIVE METHODOLOGIES FOR CRANKSHAFT OPTIMIZATION

This study involves a comprehensive methodology integrating advanced software tools to optimize the fatigue life and stress analysis of a single-cylinder four-stroke crankshaft. SolidWorks facilitated the precise design of the crankshaft, piston, and connecting rod components, enabling detailed three-dimensional modeling essential for accurate simulations and analyses. The selection of structural steel for the crankshaft material was based on its strength, stiffness, ease of machinability, cost-effectiveness, and fatigue resistance characteristics. Multibody dynamics analysis using ADAMS View provided crucial insights into the dynamic behavior of the crankshaft assembly during engine strokes. This software facilitated the evaluation of forces, moments, and kinematic interactions among components such as the piston, connecting rod, and crankpin. The application of analytical calculations to determine gas forces further validated our simulation results, ensuring comprehensive accuracy in our dynamic assessments.

The main aspect of the methodology is Finite Element Analysis (FEA), which was conducted using ANSYS software. This approach involved analyzing the crankshaft under varying diameters of crankpins, subjected to identical mechanical loads and operational conditions. Detailed meshing and precise boundary conditions were applied to simulate stress distribution, deformation and predict fatigue life cycles. The integration of mesh refinement with appropriate boundary conditions ensured accurate predictions of mechanical behaviors crucial for optimizing crankshaft durability and performance. Furthermore, the study incorporated an optimization process aimed at maximizing crankshaft fatigue life while minimizing weight and maintaining requisite strength. This involved iterative adjustments in design parameters based on FEA results, ensuring robustness in the final optimized design. By combining advanced simulation tools with analytical results, the study not only enhances the understanding of crankshaft performance but also contributes to advancing methodologies in engine component design and optimization.

## 3. CRANKSHAFT MODELING AND ANALYSIS

The dimensions of the crankshaft directly influence engine parameters and performance, including the compression ratio, combustion factors, efficiency, etc. Table 1 details the dimensions of the crankshaft used for analysis in this paper. A stroke length of 10 cm corresponds to a swept volume of 196.35 cm, with a piston mass of 0.1374 kg. The specific gas constant, denoted as '*R*', is 114.229 g/mol, derived from the molar mass of $C_8H_{18}$, a component of petrol. The pressure, denoted as '*P*', acting on the piston is calculated using the ideal gas equation, resulting in a value of 14.936 MPa. Consequently, the force exerted on the piston due to gas pressure can be computed using Eq. (1).

$$F_G = P \times \frac{\pi {d_P}^2}{4} = 14.935 \times 10^6 \times \frac{22 \times 0.032^2}{7 \times 4} = 12017\ N \quad (1)$$

Table 1. Components and dimensions used in the single cylinder for stroke cylinder

| No. | Components | Dimensions |
|---|---|---|
| 1. | Connecting rod | 165 mm |
| 2. | Crankshaft diameter (r) | 50 mm |
| 3. | Crankshaft length | 150 mm |
| 4. | Piston diameter | 32 mm |
| 5. | Operating temperature | $20^0$C |
| 6. | Density of material | 7801 kg/m$^3$ |
| 7. | Petrol density | 700 kg/m$^3$ |
| 8. | Fatigue factors for bending $K_b$ | 2 |
| 9. | Fatigue factors for torsion $K_t$ | 1.5 |
| 10. | Lengths between the bearings L | 106 mm |
| 11. | Modulus of elasticity E | 210 GPa |

### 3.1 Crankshaft Load Calculation Due to Gas Force Using ADAMS View Software

The gas force on the piston is generated as a downward force of 12017 N (Equation 1) to initiate the motion. The system is subjected to a crankshaft rotational velocity of 18000 deg/s (3000 rpm). The gravitational acceleration is considered to be 9.81 m/s$^2$. The crankshaft system has many joint types, including translational joints, fixed joints, and revolute joints. Figure 1 shows the boundary conditions set for the system's multibody simulation.

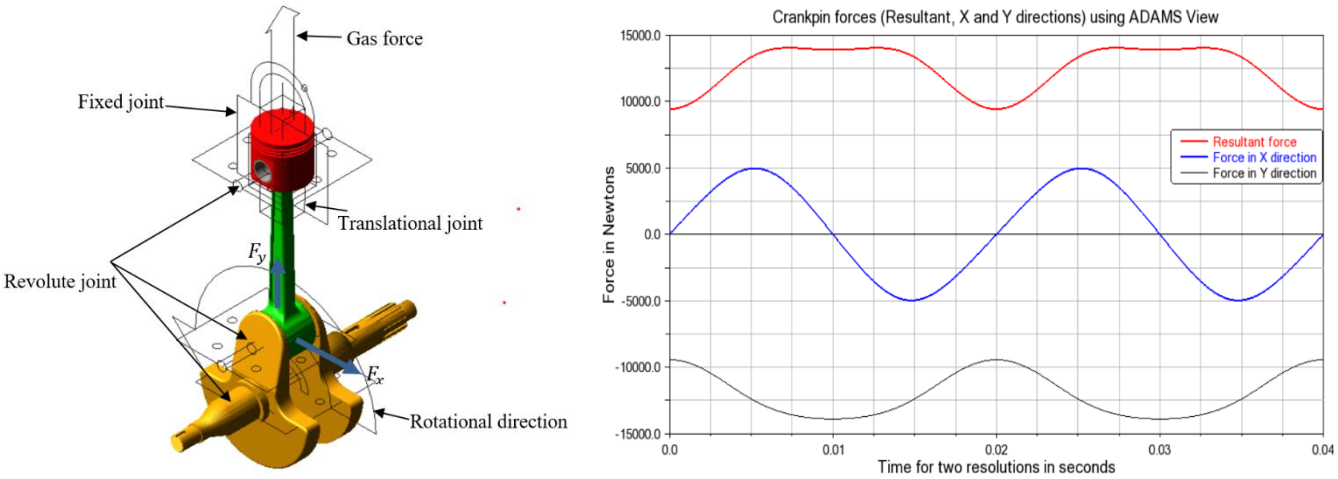


(a) (b)

Figure 1. Crankshaft: (a) with Connecting Rod and Piston in ADAMS View and (b) Force on Crankpin for Two Revolutions at 3000 RPM

Table 2. Crankpin force simulation results at 3000 RPM and 14.9 MPa cylinder pressure

| Angle in Degrees | Time (ms) | Crankpin Force Magnitude (N) | Crankpin Force in Y Direction (N) | Crankpin Force in X Direction (N) |
|---|---|---|---|---|
| 0 | 0 | 9437 | -9435 | 4 |
| 36 | 2 | 10424 | -10094 | 2594 |
| 72 | 4 | 12493 | -11622 | 4575 |
| 108 | 6 | 13860 | -13000 | 4792 |
| 131 | 7 | 14049 | -13522 | 3790 |
| 144 | 8 | 14020 | -13702 | 2935 |
| 180 | 10 | 13903 | -13895 | 5 |
| 216 | 12 | 14017 | -13702 | -2923 |
| 252 | 14 | 13854 | -12999 | -4780 |
| 288 | 16 | 12488 | -11621 | -4564 |
| 324 | 18 | 10422 | -10094 | -2585 |
| 360 | 20 | 9437 | -9437 | 4 |

Table 2 presents the calculated force acting on the crankpin at an engine speed of 3000 RPM and a cylinder pressure of 14.9 MPa. The force exerted on the crankpin is calculated for an entire cycle. The table also includes the crankpin force and its vertical (Y) and horizontal (X) components. The values were obtained through simulation using ADAMS View software and related to the components shown in Figure 1. Based on the ADAMS View simulation results shown in Table 2, it can be observed that the initial peak value of the crankpin force was at an angle of 131 degrees, which took place within a time interval of 0.00728 seconds.

### 3.2 Verification of Crankpin Force

Before the verification process, the results of the analytical calculation are compared to the results from the FEA simulation. Calculating the crankpin force from the gas force is an essential aspect of engine design and analysis. In this calculation part, several important parameters are considered. The mass of the piston with the wrist pin is 117.31 grams. The connecting rod, which has a mass of 324.86 grams and a length of 165 mm, plays a significant role in transferring the force to the crankpin of the crankshaft of the engine. Additionally, the crank, with a radius of 50 mm, helps to determine the total stroke length of the piston. Finally, the piston radius is 32 mm.

To calculate the mass distribution of the connecting rod, the rod is divided into two portions based on the position of the center of gravity as the piston end $m_1 = 120.40$ grams and the crank end $m_2 = 204.44$ gram. The piston end of the connecting rod is the portion that is attached to the piston, while the crank end is the portion that is attached to the crankshaft. The magnitude of the force exerted by the gas is given as follows;

$$F_G = P \times \frac{\pi {d_P}^2}{4} = 12017\ N$$

When applying Newton's second law of motion, the inertial force ($F_I$) arising from the reciprocating mass of $(m_p + m_1)$ at an acceleration of $a_p$ can be expressed as $(m_p + m_1)a_p$.

$$F_I = (m_p + m_1) r\omega^2 \left(cos\ \theta + \frac{cos\ 2\theta}{n}\right) = 1705 \left(cos\ \theta + \frac{cos\ 2\theta}{n}\right) \quad (2)$$

Piston effort is represented by $F_P$,

$$F_P = F_G - F_I + (m_p + m_1) g$$

The tangential force on the crank is given by $F_T$,

$$F_T = F_P \left(\sin\theta + \frac{\sin 2\theta}{2\sqrt{3.3^2 - sin^2\theta}}\right) + 2.005 \sin\theta \quad (3)$$

The radial force on the crank is given by $F_R$,

$$F_R = F_P \left(cos\ \theta - \frac{sin^2\ \theta}{\sqrt{3.3^2 - sin^2\theta}}\right) + 2.005\, cos\ \theta - 1009 \quad (4)$$

The resultant force as denoted by $F_{Result}$,

$$F_{Result} = \sqrt{F_T^2 + F_R^2}$$

$$\sin\varphi = \frac{\sin\theta}{n}\ \&\ F_Q = F_P / \cos\varphi$$

Components in the vertical upward directions,

$$F_V = -F_Q \cos\varphi + m_2 r\omega^2 \cos\theta - 9.81 m_2 \quad (5)$$

Components in the horizontal directions,

$$F_H = F_Q \sin\varphi + m_2 r\omega^2 \sin\theta \quad (6)$$

The MATLAB software was utilized to generate a plot of $F_{Result}$, $F_V$, and $F_H$ versus θ, which is illustrated in Figure 2. Table 3 shows the analytically calculated crankpin force and its components in the X and Y directions. The calculations were performed using MATLAB for accurate computation of complex equations, and the results were validated against simulation data. The values in this table are illustrated in Figure 2, which shows the resultant crankpin force and its components in the X and Y directions.

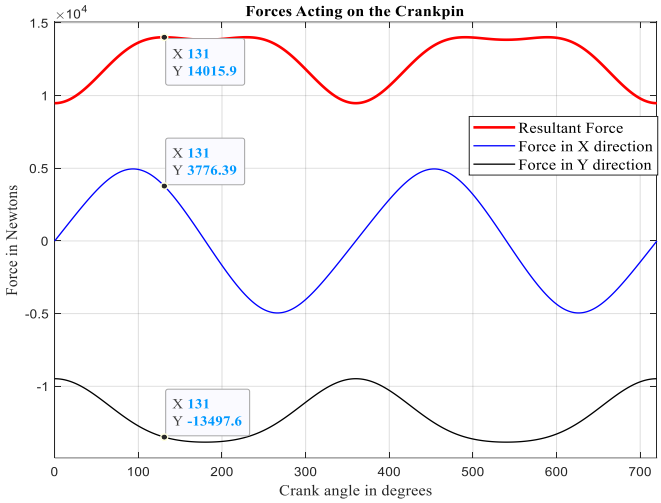


Figure 2. Crankpin force resultant and its vertical and horizontal components

Table 3. Analytical calculation of crankpin force and components in X and Y directions

| Angle in Degrees | Time (ms) | Crankpin Force Magnitude (N) | Crankpin Force in Y Direction (N) | Crankpin Force in X Direction (N) |
|---|---|---|---|---|
| 0 | 0 | 9479 | -9479 | 0 |
| 36 | 2 | 10463 | -10141 | 2576 |
| 72 | 4 | 12489 | -11630 | 4553 |
| 108 | 6 | 13828 | -12978 | 4771 |
| 131 | 7 | 14016 | -13498 | 3776 |
| 144 | 8 | 13980 | -13672 | 2920 |
| 180 | 10 | 13843 | -13843 | 0 |
| 216 | 12 | 13980 | -13672 | -2920 |
| 252 | 14 | 13828 | -12978 | -4771 |
| 288 | 16 | 12489 | -11630 | -4553 |
| 324 | 18 | 10463 | -10141 | -2576 |
| 360 | 20 | 9479 | -9479 | 0 |

The initial peak value of the crankpin force was observed at an angle of 131 degrees, which took place within a time interval of 0.00728 seconds. The crankpin force obtained through ADAMS View is validated with the results obtained from analytical calculations. An analytical approach was used to calculate the crankpin forces, and a multibody dynamics analysis was conducted using ADAMS View software.

$$\text{Error} = \frac{|\text{Analytical Value} - \text{Adams simulation measured value}|}{\text{Analytical Value}} \times 100\% \quad (7)$$

Table 4. Comparison of crankpin force using analytical method and ADAMS simulation

| Angle in Degrees | Time (ms) | Error of Crankpin Resultant Force | Error of Crankpin Force in Y Direction | Error of Crankpin Force in X Direction |
|---|---|---|---|---|
| 0 | 0 | 0.44 | 0.00 | 0.46 |
| 36 | 2 | 0.37 | 0.70 | 0.46 |
| 72 | 4 | 0.03 | 0.48 | 0.07 |
| 108 | 6 | 0.23 | 0.44 | 0.17 |
| 131 | 7 | 0.24 | 0.18 | 0.37 |
| 144 | 8 | 0.29 | 0.51 | 0.22 |
| 180 | 10 | 0.43 | 0.00 | 0.38 |
| 216 | 12 | 0.26 | 0.10 | 0.22 |
| 252 | 14 | 0.19 | 0.19 | 0.16 |
| 288 | 16 | 0.01 | 0.24 | 0.08 |
| 324 | 18 | 0.39 | 0.35 | 0.46 |
| 360 | 20 | 0.44 | 0.00 | 0.46 |

The comparison of crankpin forces between the analytical method and the Adams View-based simulation method reveals certain discrepancies when taking into account the error terms as stipulated in Eq. (7). As in Table 4, it was observed that there were minor deviations between the two methods. However, the similarities between the results confirm the validity of the force acting on the crankpin.

### 3.3 Determination of Force Components for FEA Input

In the ANSYS simulation, we analyzed the force mentioned above by determining both its tangential and radial components. The resulting values of $F_{Result}$, $F_T$ and $F_R$ were plotted against θ using MATLAB, as illustrated in Figure 3.

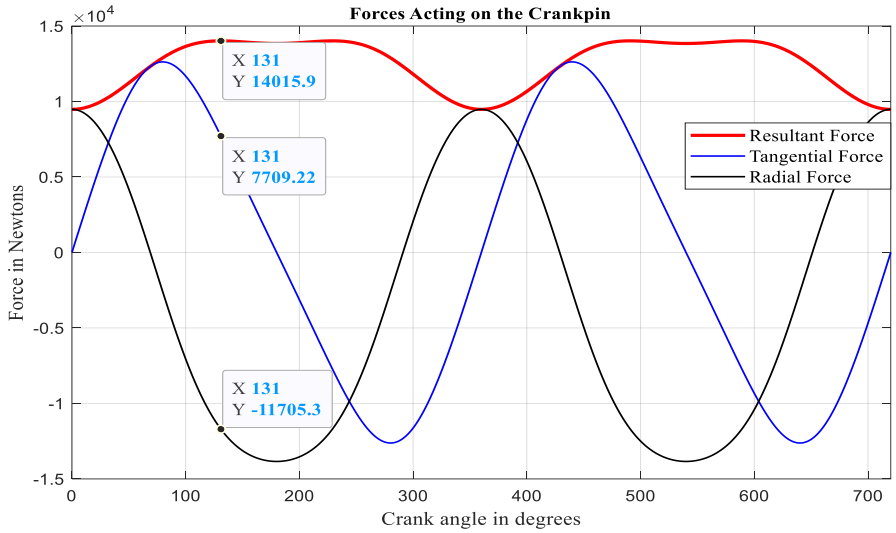


Figure 3. Crankpin force along with its tangential and radial components

This force is the resultant of a tangential force component ($F_T$) of 7,709 N and a radial force component ($F_R$) of -11,705 N.

## 4. FINITE ELEMENT ANALYSIS OF THE CRANKSHAFT

In order to carry out the FEA optimization using ANSYS, the crankshaft's material was defined as structural steel. There are three objectives to be achieved by the optimization; reducing the weight of the crankshaft structure, improving the fatigue life of the crankshaft, and reducing the manufacturing costs. The meshing model utilized in this analysis comprises 90743 nodes and 51327 elements. Within the domain of FEA, various simplifications were employed during simulations. These encompassed assuming uniform force distribution, neglecting frictional effects, presuming symmetrical bearing forces, and maintaining a constant temperature distribution throughout the crankshaft's action. Material properties were approached with linearity and isotropy, while the crankshaft was assumed to possess a homogeneous composition. Importantly, the maximum resultant force at the crankpin amounted to 14016 N, consisting of tangential and radial components measuring 7709 N and 11705 N, respectively.

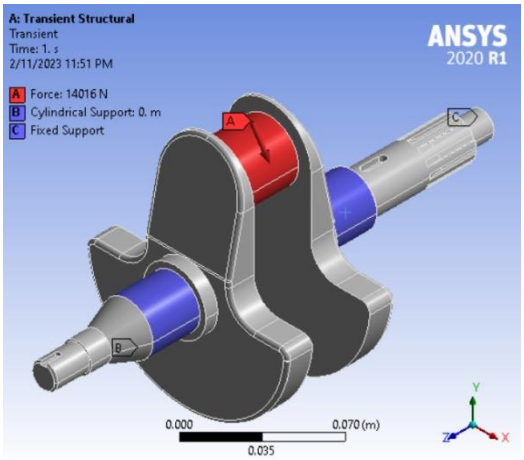


Figure 4. Boundary conditions of the crankshaft

Considering the initial and boundary conditions, as mentioned in Figure 4 and conducting ANSYS simulations at different crankpin diameters, the optimal size of the crankshaft can be determined for a given application. FEA is a valuable tool for assessing critical factors such as maximum stress, deformation, safety factors, and potential lifecycle

variations across a range of crankpin diameters. This analysis provides designers with the tools needed to make informed decisions and choose the optimal crankpin size for their design.

### 4.1 First Optimization for Crankpin Diameter 35mm

In the first optimization of the crankshaft, the crankpin diameter is defined at 35 mm. To interpret ANSYS results for von Mises stress, it is compared the maximum value with the yield strength of the material. If von Mises stress exceeds the yield strength, there is a risk of failure. The maximum von Mises stress in Figure 5(a) is lower than the yield strength of structural steel, indicating that the system is operating within safe limits. In Figure 5(d), the ANSYS results indicate a minimum safety factor of 0.8697, which is below the acceptable threshold of 1. This suggests that the structure is at risk of failure under given loading conditions, and modifications to the design are necessary to increase the safety factor to an acceptable level. The fatigue sensitivity analysis chart in Figure 5(e) illustrates the maximum cycles the crankshaft can withstand before failure, estimated at 380,030 cycles. This analysis, conducted using ANSYS FEA, focuses on how design parameters impact the crankshaft's predicted fatigue life. The x-axis details the loading history, encompassing variations in mechanical loads applied during simulations. Meanwhile, the y-axis represents available life in cycles, predicting the number of load cycles before potential fatigue failure.

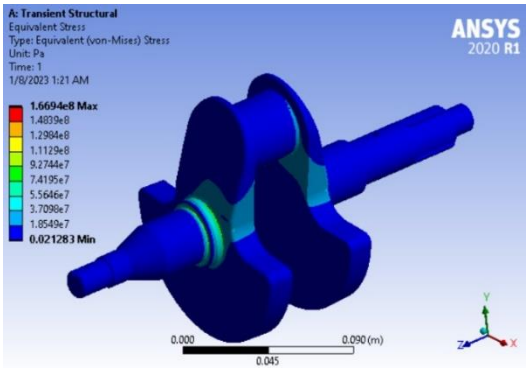


(a) Von–Mises stress

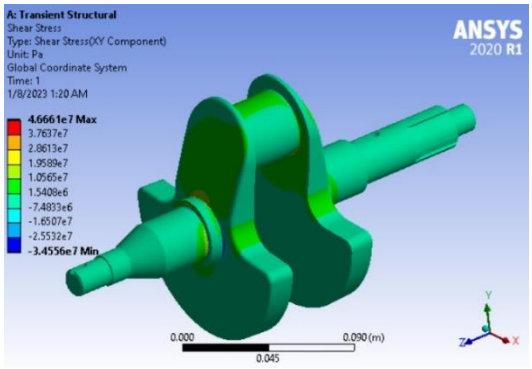


(b) shear stress analysis

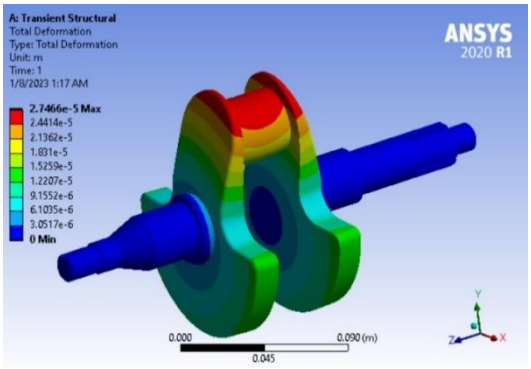


(c) total deformation

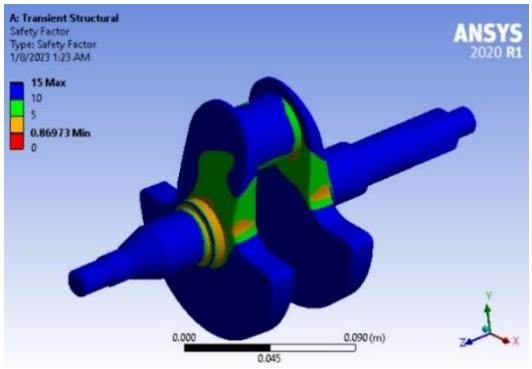


(d) safety factor

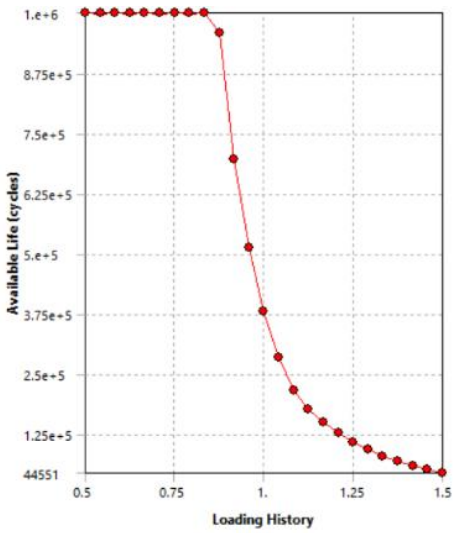


(e) number of cycles to failure

Figure 5. ANSYS analysis for crankpin diameter 35 mm

### 4.2 Geometrical Changes in the Crankshaft

To analyze a crankshaft using Finite Element Analysis (FEA), its geometric variations are studied while keeping the same material properties, loading and conditions as used before. By utilizing FEA, it is possible to optimize the crankshaft's design by analyzing various modifications and assessing their impact on geometric changes [23 – 31]. To achieve this optimization, we change the crankpin diameter by creating a hollow crankpin using SolidWorks and conducting FEA analysis with ANSYS, as illustrated in Figure 6.

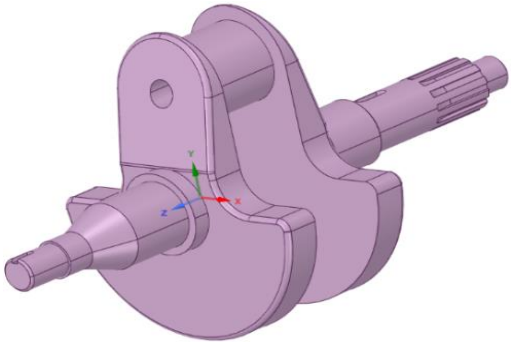

Figure 6. Modified crankshaft with inner and outer crankpin diameters

The design optimization process involves modifying the diameter sizes of the crankshaft's crankpin, encompassing both the hollow and solid versions. These optimizations, including those related to the hollow crankpin shown in Figure 6, necessitate performing the same FEA analysis previously conducted for the solid crankpin crankshaft. There is no requirement to repeat the Multibody Dynamics Analysis using ADAMS View Simulations, as all other details remain unaltered. Parameters such as von Mises stress, total deformation, shear stress, sensitivity analysis, and safety factor are computed for the optimized design of the initial crankshaft. To advance the optimization process, the crankpin diameters were modified by creating hollow crankpins with internal and external diameters, as shown in Figure 7. Subsequently, based on these ideas, FEA simulations using ANSYS were carried out to explore a range of crankpin diameters, as in Table 5.

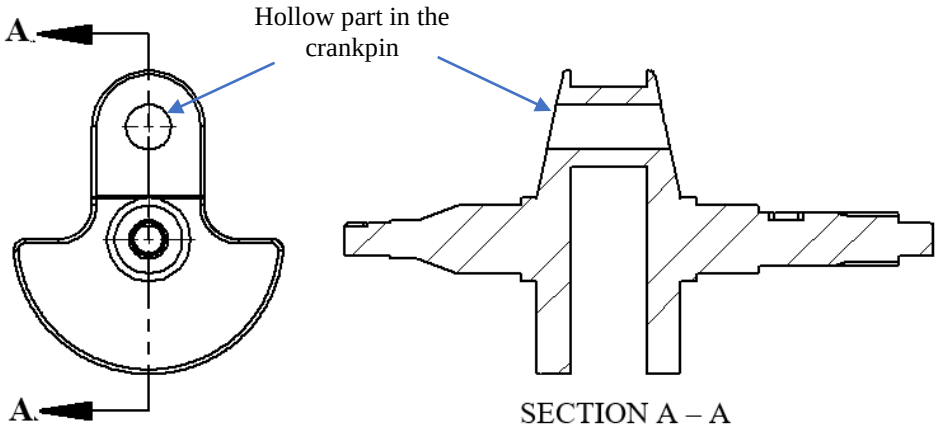


Figure 7. 2D image of modified crankshaft

Table 5. Crankpin diameters for FEA simulation

| Set of alterations | Outer diameter (mm) | Inner diameter (mm) |
|---|---|---|
| Second set of optimizations | 35 | 8 |
| | 35 | 10 |
| | 35 | 12 |
| | 35 | 14 |

### 4.3 Optimization of Crankpin Outer Diameter 35 mm and Inner Diameters 8, 10, 12 and 14 mm

In the second optimization of the crankshaft, the optimization process was similar to the previous optimizations. The outer diameter is kept fixed at 35 mm, while the inner diameters are set at 8 mm, 10 mm, 12 mm, and 14 mm, respectively.

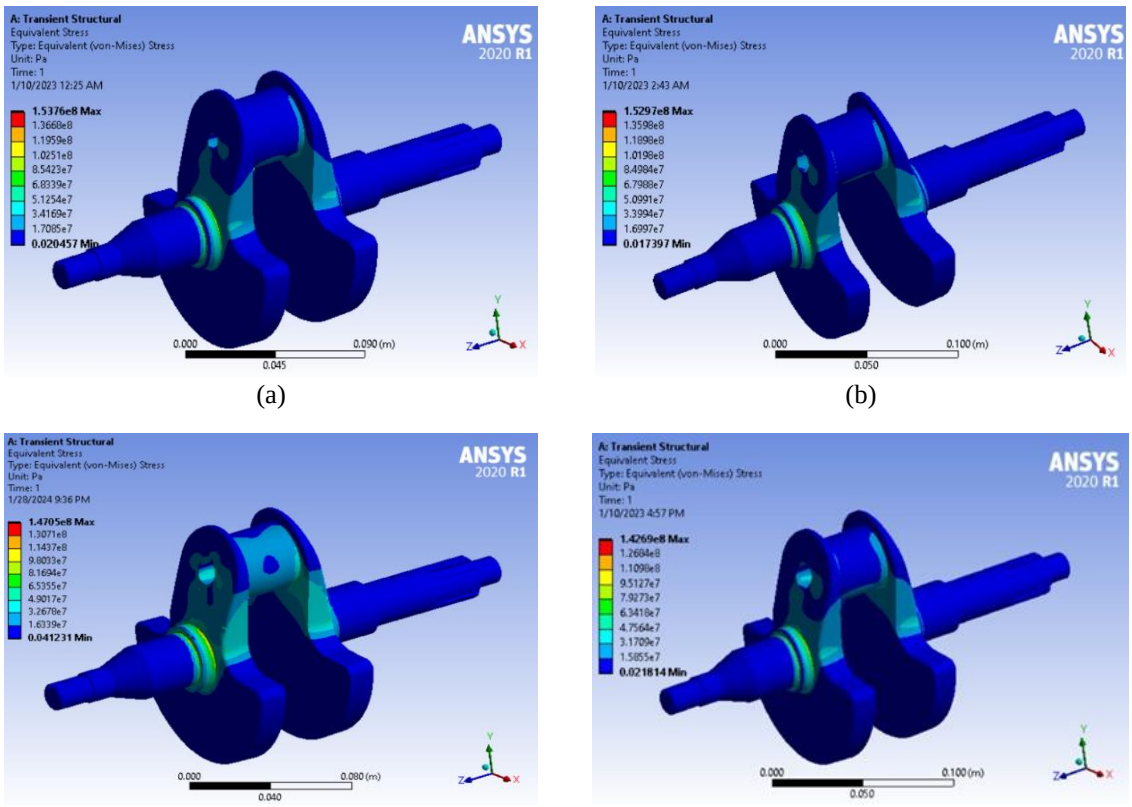


Figure 8. Von Mises stress for crankpin diameter 35/8, 35/10, 35/12 and 35/14mm

Among the crankshaft configurations investigated, the 35/14 mm design stands out with optimal characteristics in terms of von Mises stress. The FEA analysis using ANSYS shows a von Mises stress value of 142.69 MPa for this specific configuration.

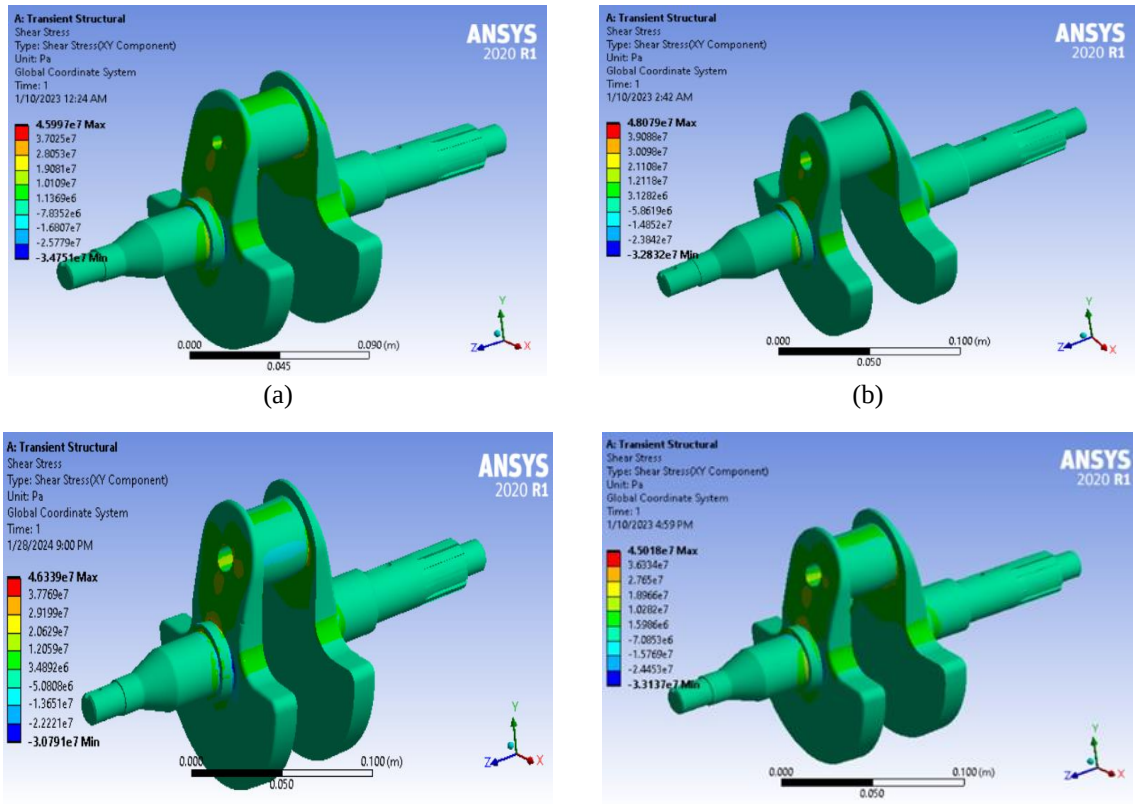


Figure 9. Shear stress for crankpin diameter 35/8, 35/10, 35/12 and 35/14mm

Among the four designs under consideration, the FEA analysis using ANSYS reveals a minimum shear stress of 45.018 MPa for the 35/14 mm crankpin diameter.

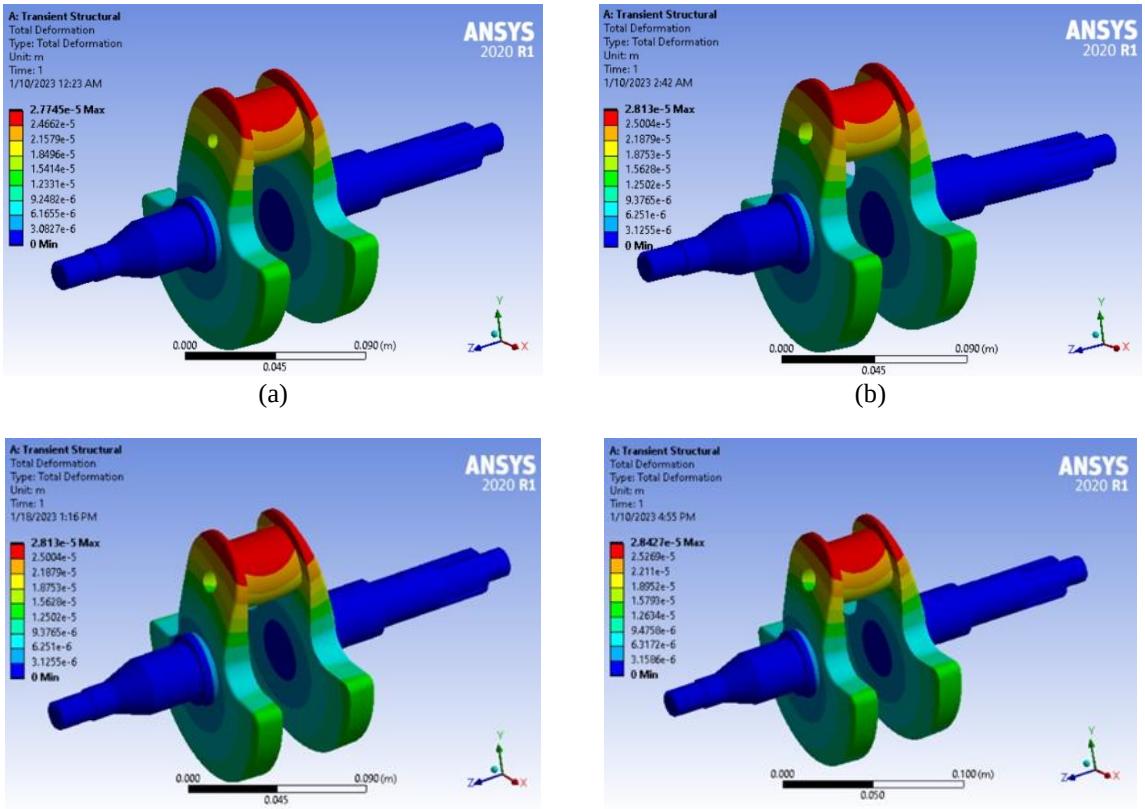


Figure 10. Total deformation for crankpin diameter 35/8, 35/10, 35/12 and 35/14mm

The ANSYS total deformation plots illustrate how different crankshaft configurations respond structurally to applied loads. These plots display deformations for crankpin diameters ranging from 35/0 to 35/14 mm, highlighting areas of strain through color gradients.

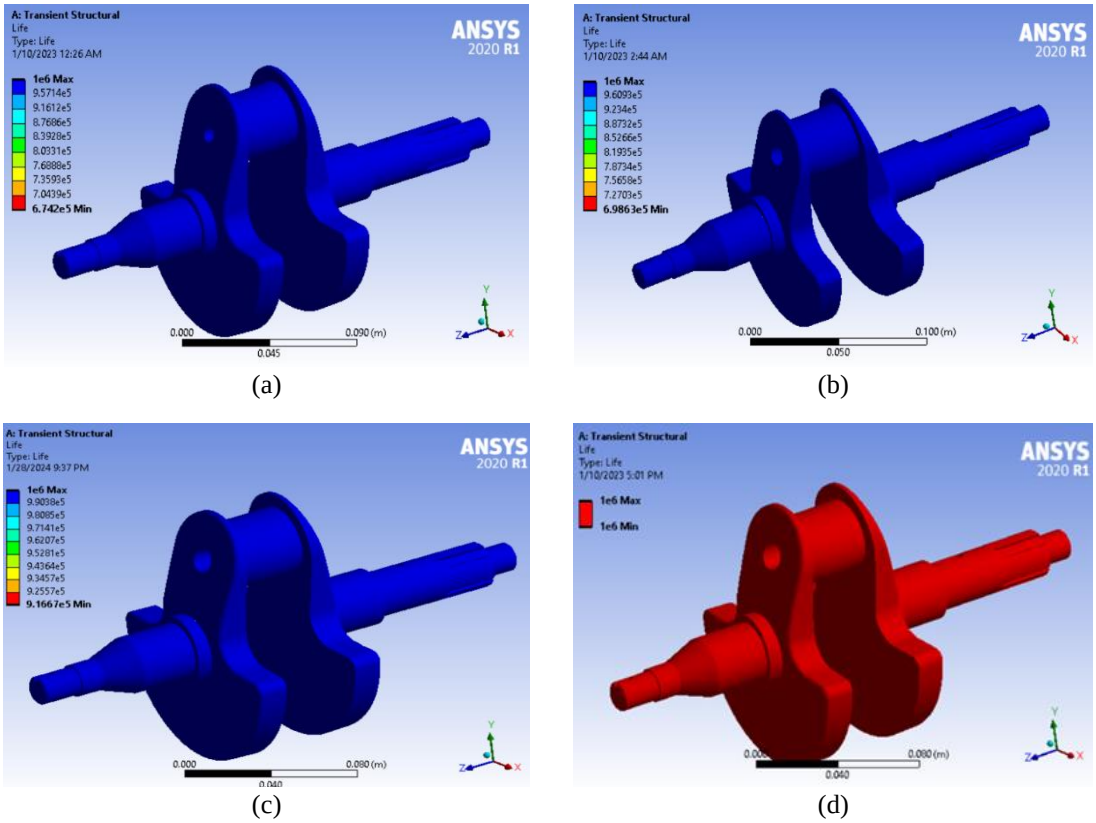


Figure 11. Life for crankpin diameter 35/8, 35/10, 35/12 and 35/14mm

Similarly, concerning fatigue life results, the 35/14 mm configuration shows a remarkable accomplishment, unveiling a fatigue life of 1,000,000 cycles. This significant outcome confirms the reliability and endurance of the 35/14 mm design. Under different crankpin diameters, the safety factor values range from 15 (Max.) – 0.86973 (Min.) to 15 (Max.) – 1.0175 (Min.). These values provide insights into the safety margins for each crankshaft configuration.

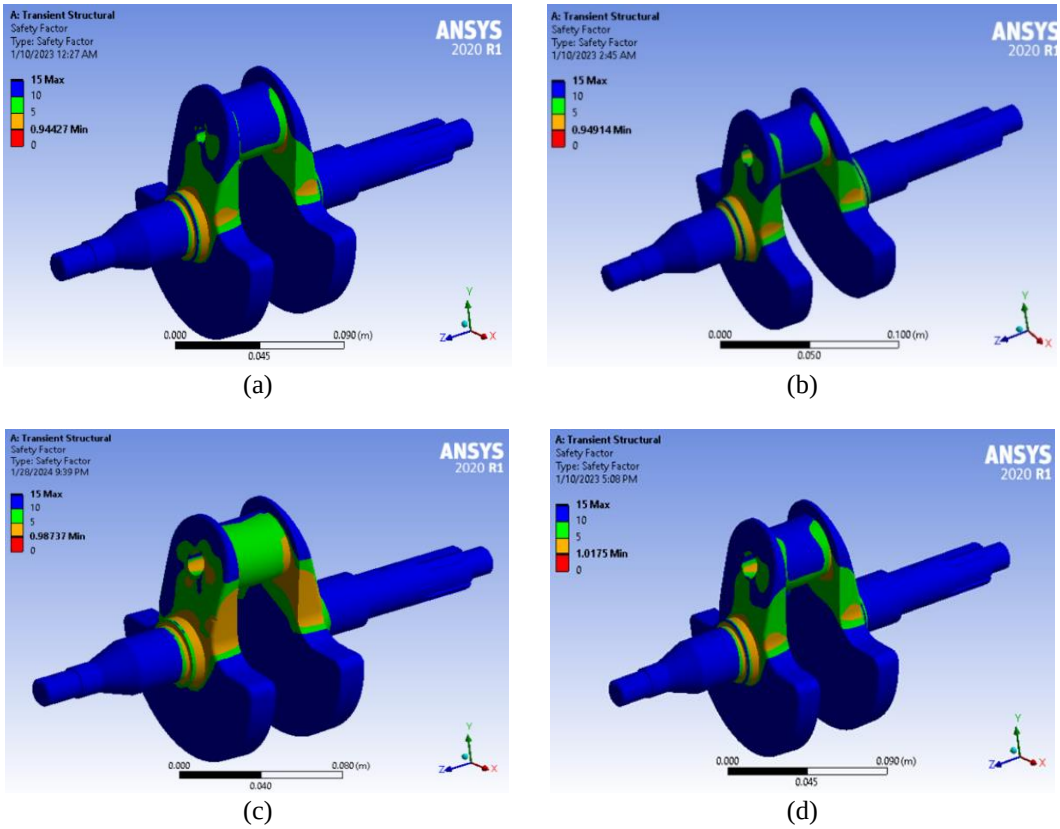


(a) (b)

(c) (d)

Figure 12. Safety factor for crankpin diameter 35/8, 35/10, 35/12 and 35/14mm

The second optimization results, shown in Figure 13(d), highlight that the fatigue life obtained is $10^6$, representing the infinite available cycles before failure. The minimum safety factor is 1.0175, which is above the acceptable threshold of 1. The third optimization of the design resulted in an increased fatigue life with a maximum number of cycles before failure and an increased value of the minimum safety factor, helping to decrease the risk of failure.

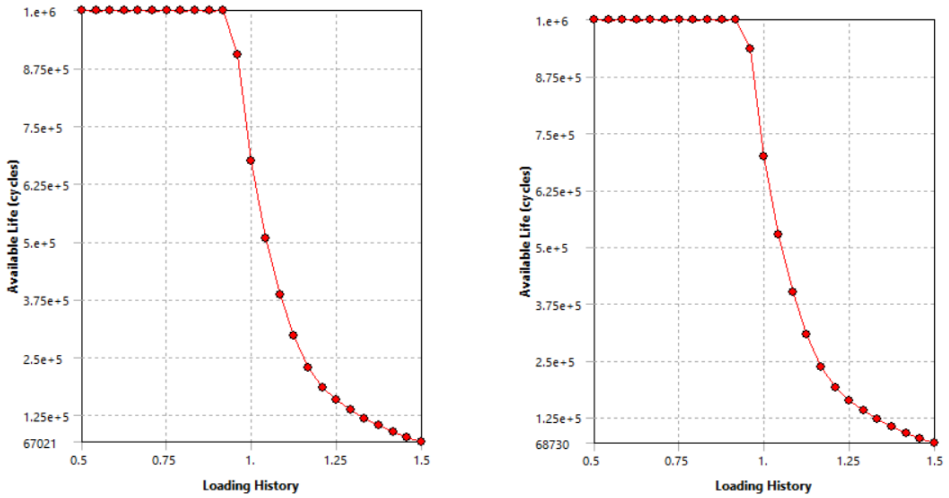


(a) (b)

Figure 13. Fatigue sensitivity for crankpin diameter 35/8, 35/10, 35/12 and 35/14mm

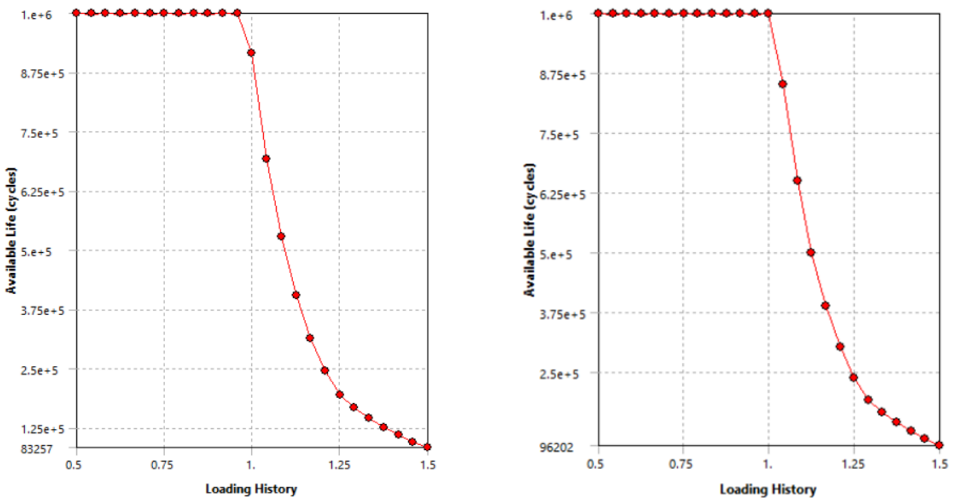


(c) (d)

Figure 13. (cont.)

### 4.4 Recommendation of the Results

The optimization process enhances understanding of the impact of fatigue life on both the inner and outer diameters of the crankpin. Results reveal that the feasible and optimal combination is an outer diameter of 35 mm and an inner diameter of 14 mm, as indicated in Table 6. This configuration yields the highest number of cycles before failure while maintaining maximum stress and shear stress within acceptable limits for structural steel. Additionally, the results are substantiated and validated through analytical calculations and Finite Element Analysis.

The result of the 35/14 mm crankpin diameter is analyzed in detail. The von Mises stress and shear stress are found to be lower than the other combinations of diameters in this analysis, as shown in Table 6, and better results were obtained than those obtained by the solid crankpin, which was analyzed before. The sensitivity analysis results significantly influence fatigue life. Changing the inner diameter of the crankpin has a greater effect than altering the outer diameter of the crankshaft. The minimum safety factor values for each are obtained from the analysis, and an improvement was found from 0.94427 to 1.0175, which implies that the lowest margin is above 1 for the crankpin diameter 35/14 mm. The process shows that the largest crankpin internal diameters give a better fatigue life for the crankshaft. The graphical representation of the results shown in Table 6 is presented in Figure 14.

Table 6. Summary of FEA results in second set of optimization

| | Parameter | Crankpin diameter 35 mm hollow diameters in mm | | | |
|---|---|---|---|---|---|
| | | 8.0 | 10.0 | 12.0 | 14.0 |
| 1 | Cycles to failure | 674200 | 698630 | 916670 | $10^6$ |
| 2 | von Mises (MPa) | 153.76 | 152.97 | 147.05 | 142.69 |
| 3 | Shear (MPa) | 45.997 | 48.079 | 46.339 | 45.018 |
| 4 | Deformation (m) | $2.7745 \times 10^{-5}$ | $2.803 \times 10^{-5}$ | $2.813 \times 10^{-5}$ | $2.8427 \times 10^{-5}$ |
| 5 | Safety Factor | 15(Max.)<br>0.94427(Min.) | 15(Max.)<br>0.94914(Min.) | 15(Max.)<br>0.9874(Min.) | 15(Max.)<br>1.0175(Min.) |

After the third optimization, the crankshaft was found to have a reduced weight and an extended fatigue life, with an optimized crankpin diameter of 35/14 mm. The crankshaft weighs 2907.36 grams and has been simulated for an infinite number of cycles. The weight reduction achieved through optimization is 2.5%, resulting in lower material costs and decreased inertial effects as well. Another graph was created to visualize the variations in the number of cycles with different crankpin diameters. Table 7 presents the values for the number of cycles to failure obtained for the entire diameter range analyzed using ANSYS. Figure 15 illustrates these variations, confirming that the best fatigue life is achieved with a 35/14 mm diameter crankpin.

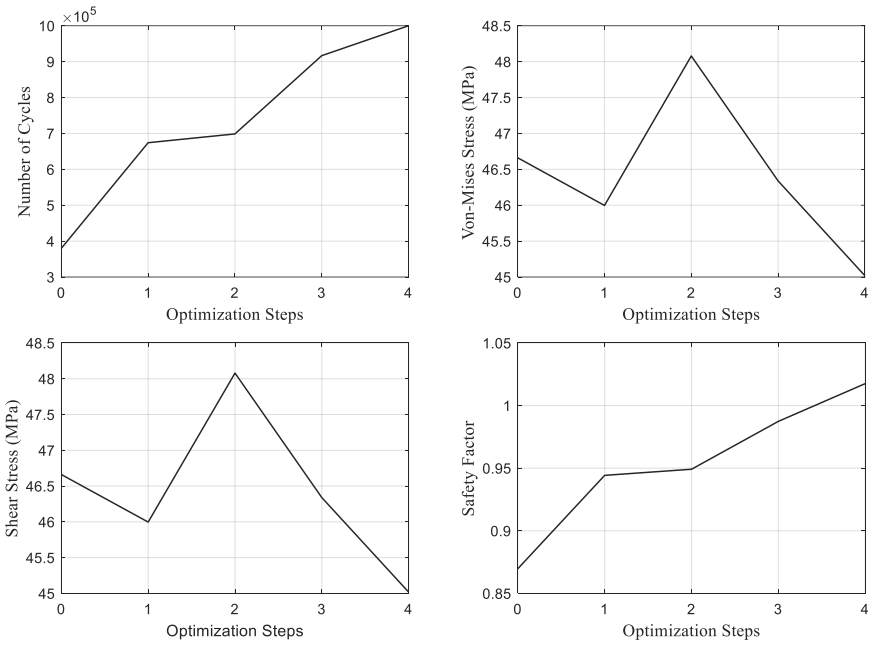


Figure 14. Graphical representation of FEA analysis of the second set

Table 7. Summary of number of cycles to failure

| Crankpin Diameters (mm) | Number of Cycles to Failure (cycles) |
|---|---|
| 35/0 | 380030 |
| 35/8 | 674200 |
| 35/10 | 698630 |
| 35/12 | 916670 |
| 35/14 | 1000000 |

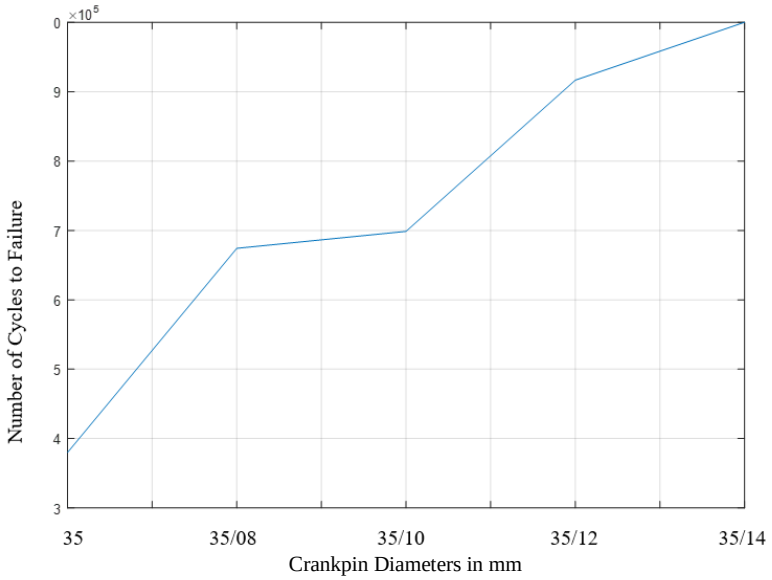


Figure 15. Cycles to failure vs crankpin diameters

The von Mises stress and maximum shear stress for the crankshaft with the crankpin diameter of 35/14 mm is obtained as the lowest value in the analysis. For a reliable operation, the value of the safety factor should be between one and fifteen. The crankshaft with the crankpin diameter of 35/14 mm is found to be the most acceptable range of safety factor value with the least weight. The final optimized crankshaft is found at a 35/14 mm crankpin diameter.

## 5. CRANKSHAFT STRESS CALCULATIONS AND VERIFICATIONS

The verification process involved comparing the FEA results with analytical calculations, focusing on stress distributions, deformation patterns, and fatigue life predictions of the crankshaft under varying operational conditions. Graphical representations have been added to illustrate the correlation between simulated and analytically calculated values. Additionally, detailed tables have been included to present numerical comparisons of stress levels, deformation characteristics, and other relevant mechanical behaviors observed during the simulation.

### 5.1 Analytical Calculations of Maximum Von – Mises Stresses and Max. Shear Stresses

Figure 2, generated using MATLAB and based on analytical equations, shows that the maximum resultant force is 14016 N at an angle of 131 degrees. Additionally, the tangential force component is 7709 N, and the radial component is -11705 N. To determine the maximum bending moment and twisting moment, it's essential to calculate the forces acting on the bearings due to these components. The distance between the bearings, '*b*', is 106 mm, the crank radius, '*r*', is 50 mm, and the crankpin diameter, '$d_c$', measures 35 mm with a length of 34 mm. The Young modulus E is 207 GPa.

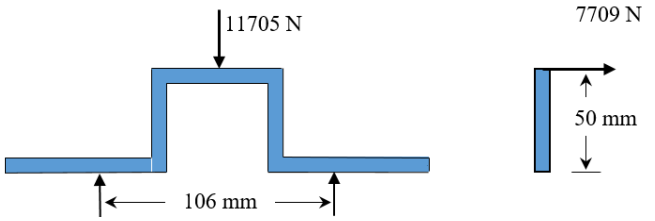


(a) Radial components (b) Tangential components

Figure 16. Free body diagram of simplified crankshaft

As a result of the radial force, the bearings experience reactions denoted as $H_{R1} and\ H_{R2}$. These reactions are equivalent and evenly distribute the radial force, indicating that each reaction carries half of the radial force. The bending moment of the crank is represented by the equation:

$$M_C = H_{R1} \times b \tag{8}$$

When subjected to the tangential force, the bearings undergo reactions referred to as $H_{T1}$ and $H_{T2}$. These reactions are equivalent and evenly distribute the tangential force, indicating that each reaction carries half of the tangential force.

The twisting moment of the crank $T_C$

$$T_C = H_{T1} \times r \tag{9}$$

The equivalent twisting moment is represented by the equation:

$$T_{eq} = \sqrt{T_c^2 + M_C^2} \tag{10}$$

Shear stress induced in the crankpin is $\tau$

$$\tau = \frac{16\, T_{eq}}{\pi\, dc^3} \tag{11}$$

Section modulus of the crankpin is denoted as z,

$$z = \frac{\pi}{32} d_c^3 \tag{12}$$

The equation represents the equivalent bending moment:

$$M_{eq} = \sqrt{(K_b \times M_c)^2 + \frac{3}{4}(K_t \times T_c)^2} \tag{13}$$

$K_b$ and $K_t$, represent the fatigue factors for bending and torsion with values of 2 and 1.5, respectively.

Von–Mises stress induced in the crankpin is represented as $\sigma_{von}$.

$$\sigma_{von} = \frac{M_{eq}}{z} \tag{14}$$

Maximum deformation $\delta$

$$\delta = \frac{\sigma_{von}\, L}{E} \tag{15}$$

As a result of the radial force, the reaction at each bearing is $5852.5\ N$ which gives the bending moment of 310.18 N.m. Also, due to the tangential force, the reaction at the bearing is 3854.5 N with a twisting moment of 192.73 N.m.

Both of these moments generate the equivalent twisting moment of 365.18 N.m and the shear stress of 43.379 MPa. Therefore, the equivalent bending moment of the crankshaft is $668.98\ MPa$. The von Mises stress and maximum deformations are determined to be 158.93 MPa and $2.61044 \times 10^{-2}$ mm, respectively. These calculations are based on the crankpin's section modulus, which measures $4.2092 \times 10^{-6}$ mm$^3$.

Table 8. Summary of analytical results for crankpin

| Parameters | Crankpin inner diameter in mm (Outer 35mm) | | | |
|---|---|---|---|---|
| | 8.0 | 10.0 | 12.0 | 14.0 |
| Max. Von – Mises stress (MPa) | 160.860 | 161.730 | 162.610 | 163.400 |
| Max. Shear stress (MPa) | 43.904 | 44.415 | 45.201 | 46.346 |
| Max. Deformation (m) | $2.64207 \times 10^{-5}$ | $2.67286 \times 10^{-5}$ | $2.72015 \times 10^{-5}$ | $2.78902 \times 10^{-5}$ |

### 5.2 Results Comparisons

The FEA Analysis results of the maximum of von Mises stresses, shear stresses and deformations are compared with the analytically calculated results among the different designs of the same crankshaft with the same operating conditions.

Table 9. FEA analysis comparisons of the crankpin

| Parameters | | (Outer Dia. 35mm) Crankpin inner diameters in mm | | | | |
|---|---|---|---|---|---|---|
| | | 0.0 | 8.0 | 10.0 | 12.0 | 14.0 |
| Max. von – Mises stress (MPa) | FEA | 166.94 | 153.76 | 152.97 | 147.05 | 142.69 |
| | Analytical | 158.93 | 160.86 | 161.73 | 162.61 | 163.40 |
| | Error % | 4.80% | 4.62% | 5.73% | 10.58% | 14.58% |
| Max. shear stress (MPa) | FEA | 46.661 | 45.997 | 48.079 | 46.339 | 45.018 |
| | Analytical | 43.379 | 43.904 | 44.415 | 45.201 | 46.346 |
| | Error % | 6.83% | 4.50% | 7.62% | 2.46% | 2.76% |
| Max. deformation (m) | FEA | $2.7466 \times 10^{-5}$ | $2.7745 \times 10^{-5}$ | $2.803 \times 10^{-5}$ | $2.813 \times 10^{-5}$ | $2.8427 \times 10^{-5}$ |
| | Analytical | $2.6104 \times 10^{-5}$ | $2.64207 \times 10^{-5}$ | $2.67286 \times 10^{-5}$ | $2.72015 \times 10^{-5}$ | $2.78902 \times 10^{-5}$ |
| | Error % | 5.22% | 4.77% | 5.24% | 3.29% | 1.92% |

This Comparison is done for Finite Element Analysis (FEA) results with analytical results in order to validate the accuracy and reliability of FEA simulations. Both of these results differ slightly, and they ensure that the crankshaft readings are valid. In the comparisons of initial and final results, it is found that there is a better improvement in fatigue life as well as the maximum stress and shear stress value. Also, improvement in the safety factor ensures the reliability of the design. The initial and final results are compared in Table 10, which provides the details of improvements and success of the objective of this study.

Table 10. Comparing initial optimal crankshaft solutions

| | Parameter | Hollow diameters in mm | | Percentage change |
|---|---|---|---|---|
| | | 35 | 35/14 | |
| 1 | Cycles to Failure (Cycles) | 380030 | $10^6$ | Increased by 163% |
| 2 | von Mises Stress (MPa) | 166.94 | 142.69 | Decreased by 16% |
| 3 | Shear Stress (MPa) | 46.661 | 45.018 | Decreased by 3.5% |
| 4 | Deformation (m) | $2.7466 \times 10^{-5}$ | $2.8427 \times 10^{-5}$ | Increased by 3.5% |
| 5 | Safety Factor | 15(Max.)<br>0.86924(Min.) | 15(Max.)<br>1.0175(Min.) | Improved to safe range |
| 6 | Weight (gram) | 2954.05 | 2907.36 | Reduced by 1.6% |

### 5.3 Model Verification and Reliability

To ensure the acceptance of the results from this fatigue life analysis of a single-cylinder four-stroke crankshaft, it is crucial to validate their accuracy and reliability. To carry out the reliability of the results, it is important to make sure the loading conditions, types of joints, inertia effects and material properties used in the analysis which represent the actual operating conditions of the crankshaft. To ensure validation, the experimental results are validated with the analytically calculated results [32]. In some situations, the computer simulation results are compared with the analytically calculated results for validation [33]. Therefore, the results can be ensured that the outcomes are closely associated with real-world observations. Another aspect is the verification of the results, which is done through the comparison with published results [34].

### 5.4 Strengths and Weakness for the Study

The analysis of the crankshaft highlighted significant strengths in design optimization using advanced tools like SolidWorks and ANSYS. These methods effectively enhanced fatigue life and minimized weight through detailed stress analysis and simulation. However, limitations were identified. Simplifications in load distribution and bearing support conditions may affect stress predictions, while neglecting temperature variations could underestimate their impact on material fatigue. Assumptions of uniform diameter in analytical calculations might not fully reflect the crankshaft's actual mass distribution and inertial properties. Adjusting crankpin diameters for optimization poses challenges such as increased weight and manufacturing complexities. Addressing these limitations is crucial for refining future analyses and improving the accuracy of computational simulations in crankshaft design.

## 6. CONCLUSION

To conclude, the main objective of optimizing the crankshaft design using simulation methods was successfully achieved. The crankpin force during the operation was predicted through multibody dynamics simulations in ADAMS View and validated with analytical calculations. The optimization process started with finite element analysis in ANSYS for the original crankshaft design, followed by weight optimization by altering the crankpin radius. These changes reduced the crankshaft's overall weight by 2.5%, leading to lower inertia forces, cost savings, and improved engine performance. The study showed that design optimization significantly improved fatigue life, reduced material costs, and enhanced engine performance, with FEA using ANSYS saving time compared to analytical calculations.

The optimal diameter was determined through FEA simulations and analytical calculations, highlighting the impact of crankpin diameter changes on fatigue life and stress distribution. The study focused on enhancing the crankshaft's fatigue life through design optimization, specifically by adjusting the crankpin diameter. The findings, validated through simulations and calculations, showed that a 35/14 mm crankpin diameter substantially increased fatigue life and addressed stress concentration concerns, emphasizing the importance of design modifications in achieving desired outcomes.

## ACKNOWLEDGEMENTS

The authors gratefully acknowledge the support of the Faculty of Mechanical Engineering, Universiti Teknologi Malaysia, in completing this project successfully.

## CONFLICT OF INTEREST

The authors declare that they do not have any conflict of interest.

## AUTHORS CONTRIBUTION

Jayanthan: Conceptualization, methodology, writing, and data analysis.
Abu Bakar: Data curation, review, editing, visualization and supervision.
Mazali: Data curation, review, editing, and supervision.

## REFERENCES

[1] S. Pal and K.S. Surendra, "Experimental investigation on cycle time in machining of forged crankshaft," *Materials Today*, vol. 44, pp. 1469–1472, 2021.

[2] G. Ramesh, M. Dora Babu, R. Satheesh and M. Kumar, "Design static and modal analysis of crankshaft," *International Journal of Creative Research Thoughts*, vol. 6, pp. 254–261, 2018.

[3] M.C. Priyanka, and R.H. Shinde, "Design & analysis of crankshaft for single cylinder diesel engine," *International Research Journal of Engineering and Technology*, vol. 8, pp. 1311–1319, 2021.

[4] M. Fonte, V. Infante, M.J. Freitas and L. Reis, "Failure mode analysis of two diesel engine crankshafts," *Procedia Structural Integrity*, vol. 1, pp. 313-318, 2016.

[5] K. Aliakbari, N. Safarzadeh and S.S. Mortazavi, "Analysis of the crankshaft failure of wheel loader diesel engine," *International Journal of Engineering*, vol. 31, no. 3, pp. 473-479, 2018.

[6] V. Mallikarjuna, B.J. Prasad and G. Kishore, "Design and finite element analysis of crank shaft by using Catia and Ansys," *SSRG International Journal of Mechanical Engineering*, vol. 4, pp. 8-18, 2017.

[7] S. Manpreet and P.D. Dhiraj, "Materials comparison for crankshaft in Ansys," *International Journal of Management, Technology and Engineering*, vol. 9, pp. 410–414, 2019.

[8] B. Chiliński1 and M. Zawisza, " Analysis of bending and angular vibration of the crankshaft with a torsional vibrations damper," *Journal of Vibroengineering*, vol. 18, pp. 492-504, 2016.

[9] Anish, "Reasons for failure and misalignment of crankshaft in marine engines," [online] [cited 2019]. Available at: https://www.marineinsight.com/main-engine/reasons-for-failure-and-misalignment-of-crankshaft-in-marine-engines/

[10] A. Arshad, C. Pengbo, A.A.E. Elmenshawy and B. Ilmars, "Design optimization for the weight reduction of 2-cylinder reciprocating compressor crankshaft," *Achieve of Mechanical Engineering*, vol. 68, pp. 281–286, 2021.

[11] Y.Z. Ang and P.X. Ku, "Study on failure analysis of crankshaft using finite element analysis," *MATEC Web of Conferences 335*, vol. 335, pp. 233–239, 2021.

[12] L. Witek, M. Sikora, F. Stachowicz and T. Tomasz, "Stress and failure analysis of the crankshaft of diesel engine," *Engineering Failure Analysis*, vol. 82 pp. 703–712, 2017.

[13] V. Sowjanya, and C. Raghunatha Reddy, "Design and analysis of a crank shaft," *International Journal of Engineering Science and Computing*, vol. 6, pp. 3814-3821, 2017.

[14] S. Mahendrakar and P.R. Kulkarni, "A review on design and vibration analysis of a crank shaft by FEA and experimental approach," *International Journal of Scientific Development and Research*, vol. 1, pp. 146–149, 2017.

[15] V.C. Shahane and R.S. Pawar, "A review on finite element analysis of the crankshaft of internal combustion engine," *International Research Journal of Engineering and Technology*, vol. 3, pp. 1658–1663, 2016.

[16] G. Gopal, L.S. Kumar, K.V.B. Reddy, M.U.M. Rao and G. Srinivasulu, "Analysis of piston, connecting rod and crank shaft assembly," *Materials Today: Proceedings*, vol. 4, pp. 7810–7819, 2017.

[17] M. Degefe, P. Paramasivam, D. Tamana and K. Venkatesh, "Optimization and finite element analysis of single cylinder engine crankshaft for improving fatigue life," *American Journal of Mechanical and Materials Engineering*, vol. 1, pp. 58–68, 2017.

[18] M.N. Pratiksha, "Analysis of crankshaft," *International Journal of Scientific Engineering and Research*, vol. 5, pp. 2347–3878, 2017.

[19] B.G. Nandkumar, Z.S. Bhaskar and P.A. Ramesh, "Design, optimization and finite element analysis of crankshaft," *International Journal of Innovation in Engineering, Research and Technology*, vol. 15, pp.1-7, 2015.

[20] P.Thejasree, K.D. Kumar and S.L.P. Lakshmi, "Modelling and analysis of crankshaft for passenger car using Ansys," *Materials Today: Proceedings*, vol. 4, pp. 11292–11299, 2017.

[21] B.V. Ramnath, C. Elanchezhian, J. Jeykrishnan, R. Ragavendar, P.K. Rakesh, J.S Dhamodar and A. Danasekar, "Implementation of reverse engineering for crankshaft manufacturing industry," *Materials Today: Proceedings*, vol. 5, pp. 994–999, 2018.

[22] R. Pradhan and S. Puhan, "Analysis and optimization of crankshaft for a single cylinder four stroke SI engine," *Journal of Emerging Technologies and Innovative Research*, vol. 5, pp. 246–249, 2018.

[23] K.P. Durga, V.J.P. Narayana and N. Kiranmaye, "Design and stress analysis of crankshaft for single cylinder four stroke diesel engine," *International Journal of Engineering Research & Technology*, vol. 7, pp. 154-159, 2018.

[24] I.T. Jiregna, G.G. Sirata and F.T. Soramo, "Fatigue failure analysis of crankshafts - A review," *International Journal of Innovative Science, Engineering and Technology*, vol. 7, pp. 93–106, 2020.

[25] P. Citti, A. Giorgetti and U. Millefanti, "Current challenges in material choice for high-performance engine," *International Conference on Stress Analysis*, vol. 8, pp. 486–500, 2018.

[26] K. Satyanarayana, A.K. Viswanath, T.V. Hanumanta Rao and S.V. Uma Maheswara Rao, "Investigation of the stresses induced in crank shaft AISI E4340 forged steel," *11th International Symposium on Plasticity and Impact Mechanics, Procedia Engineering*, vol. 173, pp. 1672–1677, 2017.

[27] P. Mishara and S. Sinha, "Stress analysis and topology optimization of connecting rod of two wheelers using FEA," *International Journal of Mechanical Technology*, vol. 9, pp. 559–568, 2018.

[28] A. Muhammad and I.H. Shanono, "Static analysis and optimization of a connecting rod," *International Journal of Engineering Technology and Sciences,* vol. 6, pp. 24-40, 2019.

[29] S.N. Kurbet, V.V. Kuppast and T. Basavaraj, "Material testing and evaluation of crankshafts for structural analysis," *Materials Today: Proceedings*, vol. 34, pp. 556-562, 2021.

[30] T. Nageswara Rao, K. Vasudev Rao, V. Ananta Rahul, G. Rajesh, and S.S. Sowgandh, "Analysis and Optimization of Gas/petrol Engine Components," *International Journal of Latest Technology in Engineering, Management & Applied Science*, vol. 7, pp. 230-236, 2018.

[31] L. Karthick, N. Mallireddy, J. Yogaraja, S. Sivakumar, and A. Sasikumar, "Modelling and analysis of an EN8 crankshaft material in comparison with Forged steel crankshaft," *Materials Today: Proceedings*, vol. 47, pp. 6168-6172, 2021.

[32] S.S. Mohtasebi, H. Afshari and H. Monili, "Analysis of crankshafts vibrations to compare the dynamic behavior of steel and cast iron crankshafts," *Journal of Applied Sciences,* vol. 6, pp. 591-594, 2006.

[33] K. Sandya, M. Keerthi and K. Srinivas, "Modelling and stress analysis of crankshaft using FEM package Ansys," *Journal of Emerging Technologies and Innovative Research*, vol. 6, pp.378-383, 2019.

[34] R. Hamel, L. Mustapha and B. Benyebka, "Elasto-hydrodynamic lubrication analysis of a porous misaligned crankshaft bearing operating with nanolubrications," *Mechanics & Industry*, vol. 24, 2022.